Optical properties of surface plasmon resonances of coupled metallic nanorods

Elizabeth J. Smythe, Ertugrul Cubukcu, and Federico Capasso

Harvard School of Engineering and Applied Science, Harvard University, 29 Oxford St, Cambridge, Massachusetts, 02138

capasso@deas.harvard.edu

Abstract: We present a systematic study of optical antenna arrays, in which the effects of coupling between the antennas, as well as of the antenna length, on the reflection spectra are investigated and compared. Such arrays can be fabricated on the facet of a fiber, and we propose a photonic device, a plasmonic optical antenna fiber probe, that can potentially be used for *in-situ* chemical and biological detection and surface-enhanced Raman scattering.

OCIS codes: (240.6680) Surface Plasmons; (060.2370) Fiber Optic Sensors; (260.5740) Resonance.

References and links

1. S.L. Zou and G.C. Schatz, **"**Silver nanoparticle array structures that produce giant enhancements in electromagnetic fields," Chem. Phys. Lett. **403,** 62-67 (2005).
2. D.A. Genov, A.K. Sarychev, V.M. Shalaev, and A. Wei, "Resonant field enhancements from metal nanoparticle arrays," Nano Lett. **4,** 153-158 (2004).
3. N. Félidj, S. Lau Truong, J. Aubard, G. Lévi, J. R. Krenn, A. Hohenau, A. Leitner, and F. R. Aussenegg, "Gold particle interaction in regular arrays probed by surface enhanced Raman scattering," J. Chem. Phys. **120,** 7141-7146 (2004).
4. G. Laurent, N. Félidj, S. Lau Truong, J. Aubard, G. Lévi, J. R. Krenn, A. Hohenau, A. Leitner, and F. R. Aussenegg, "Imaging surface plasmon of gold nanoparticle arrays by far-field Raman scattering," Nano Lett. **5,** 253-258 (2005).
5. N. Félidj, J. Aubard, G. Lévi, J. R. Krenn, M. Salerno, G. Schider, B. Lamprecht, A. Leitner, and F. R. Aussenegg, "Controlling the optical response of regular arrays of gold particles for surface-enhanced Raman scattering," Phys. Rev. B **65,** 075419 (2002).
6. D. P. Fromm, A. Sundaramurthy, A. Kinkhabwala, P. J. Schuck, G. S. Kino, and W. E. Moerner, "Exploring the chemical enhancement for surface-enhanced Raman scattering with Au bowtie nanoantennas," J. Chem. Phys. **124,** 061101 (2006).
7. G. Laurent, N. Félidj, J. Aubard, and G. Lévi, J. R. Krenn, A. Hohenau, G. Schider, A. Leitner, and F. R. Aussenegg, "Evidence of multipolar excitations in surface enhanced Raman scattering," Phys. Rev. B **71,** 045430 (2005).
8. L. Billot, M. Lamy de la Chapelle, A. S. Grimault, A. Vial, D. Barchiesi, J. L. Bijeon, P. M. Adam, and P. Royer, "Surface enhanced Raman scattering on gold nanowire arrays: Evidence of strong multipolar surface plasmon resonance enhancement," Chem. Phys. Lett. **422,** 303–307 (2006).
9. A. D. McFarland, M. A. Young, J. A. Dieringer, and R. P. Van Duyne, "Wavelength-Scanned Surface-Enhanced Raman Excitation Spectroscopy," J. Phys. Chem. B **109**, 11279-11285 (2005).
10. K. H. Su, S. Durant, J. M. Steele, Y. Xiong, C.Sun, and X. Zhang, "Wavelength-scanned surface-enhanced Raman excitation spectroscopy," J. Phys. Chem B **110,** 3964-3968 (2006).
11. J. Grand, M. Lamy de la Chapelle, J. L. Bijeon, P. M. Adam, A. Vial, and P. Royer, "Role of localized surface plasmons in surface-enhanced Raman scattering of shape-controlled metallic particles in regular arrays," Phys. Rev. B **72** 033407 (2005).
12. E. Cubukcu, E. A. Kort, K. B. Crozier and F. Capasso, "Plasmonic laser antenna" Appl. Phys. Lett. **89**, 093120 (2006).
13. A. Sundaramurthy, P. J. Schuck, N. R. Conley, D. P. Fromm, G.S. Kino, and W. E. Moerner, "Toward Nanometer-Scale Optical Photolithography: Utilizing the Near-Field of Bowtie Optical Nanoantennas," Nano Lett. **6,** 355-360 (2006).

#82036 - $15.00 USD Received 11 Apr 2007; revised 24 May 2007; accepted 25 May 2007; published 1 Jun 2007

14. J P. Kottmann and O. J.F. Martin, "Spectral response of plasmon resonant nanoparticles with a non-regular shape," Opt. Express **6,** 213-219 (2000).
15. K. H. Su, Q. H. Wei, X. Zhang, J. J. Mock, D. R. Smith, and S. Schultz, "Interparticle Coupling Effects on Plasmon Resonances of Nanogold Particles," Nano Lett. **3,** 1087-1090 (2003).
16. Q. H. Wei, K. H. Su, S. Durant, and X. Zhang, "Plasmon Resonance of Finite One-Dimensional Au Nanoparticle Chains," Nano Lett. **4,** 1067-1071 (2004).
17. G. Schider, J. R. Krenn, A. Hohenau, H. Ditlbacher, A. Leitner, F. R. Aussenegg, W. L. Schaich, I. Puscasu, B. Monacelli, and G. Boreman, "Plasmon dispersion relation of Au and Ag nanowires," Phys. Rev. B **68,** 155427 (2003).
18. W. Rechberger, A. Hohenau, A. Leitner, J .R. Krenn, B. Lamprecht, and F.R. Aussenegg, "Optical properties of two interacting gold nanoparticles," Opt. Commun. **220,** 137–141 (2003).
19. L. J. Sherry, R. Jin, C. A. Mirkin, G. C. Schatz, and R.P. Van Duyne, "Localized Surface Plasmon Resonance Spectroscopy of Single Silver Triangular Nanoprisms," Nano Lett. **6,** 2060-2065 (2006).
20. M. D. Malinsky, K. L. Kelly, G.C. Schatz, and R. P. Van Duyne, "Nanosphere Lithography: Effect of Substrate on the Localized Surface Plasmon Resonance Spectrum of Silver Nanoparticles," J. Phys. Chem. B **105,** 2343-2350 (2001).
21. M. Danckwerts, and L. Novotny, "Optical Frequency Mixing at Coupled Gold Nanoparticles," Phys. Rev. Lett. **98,** 026104 (2007).
22. T. H. Taminiau, R. J. Moerland, F. B. Segerink, L. Kuipers, and N. F. van Hulst, "λ/4 Resonance of an Optical Monopole Antenna Probed by Single Molecule Fluorescence," Nano Lett. **7**, 28-33 (2007).
23. R. M. Stöckle, Y. D. Suh, V. Deckert, R. Zenobi, "Nanoscale chemical analysis by tip-enhanced Raman spectroscopy," Chem. Phys. Lett. **318**, 131–136 (2000).
24. J. P. Kottmann and O. J. F. Martin, "Retardation-induced plasmon resonances in coupled nanoparticles," Opt. Lett. **26**, 1096-1098 (2001).
25. E.D. Palik, *Handbook of Optical Constants* (Academic, 1985).
26. C. L. Haynes, A. D. McFarland, L. Zhao, R. P. Van Duyne, G. C. Schatz, L. Gunnarsson, J. Prikulis, B. Kasemo, and M. Käll, "Nanoparticle Optics: The Importance of Radiative Dipole Coupling in Two-Dimensional Nanoparticle Arrays," J. Phys. Chem. B **107**, 7337-7342 (2003).

1. Introduction

In recent years, surface plasmons have become an area of increased research interest. It is well known that small metallic particles can resonate with incident electromagnetic fields of certain wavelengths, giving rise to strongly enhanced near-fields [1, 2]. The latter can also result in surface-enhanced Raman scattering (SERS) and allow for the detection of very low concentrations of molecules [3-11]. Various metallic particles have been studied including dots, rods, and 'bowties' [12-14]. In these studies, the effects of particle size, scale, and surrounding refractive index have been investigated [15-20]. In addition, studies utilizing metallic nanoparticles attached to fiber tips have been used for nonlinear frequency generation [21], and the properties of fiber near-field scanning optical microscope (NSOM) probes with a λ/4 metallic antenna integrated on the tip have been characterized using single molecule florescence [22]. Tip-enhanced Raman spectroscopy has also been performed [23].

Coupling between resonating metallic particles, henceforth also named antennas, occurs when they are close together and their plasmon modes interact. This coupling results in resonances that are different from that of a single particle [24]. The distance between the antennas, as well as the strength of their individual interaction with the incident field, determines the nature of these resonances. For a given incident field, the enhanced near-fields that develop between an isolated pair of coupled metallic particles are stronger than those that exist if the latter are part of a large array of coupled antennas. However, arrays allow enhanced near-fields to be generated over large areas. Here we present a study of the effects of coupling between metallic nanorods that are arranged in large arrays. With both experiments and simulations we examine the arrays' reflection spectra in the strongly and weakly coupled regimes, as well as investigate the effect of nanorod length on the array resonances. We also propose a device, a fiber probe, in which these tunable arrays can be incorporated.

#82036 - $15.00 USD Received 11 Apr 2007; revised 24 May 2007; accepted 25 May 2007; published 1 Jun 2007

2. Device

Our proposed plasmonic device consists of an array of coupled metallic particles fabricated onto the facet of an optical fiber. This 'sculpted' end of the fiber can be inserted in a material or system of interest, and the other end can be connected to a signal input/output detection scheme. The fabricated arrays have a certain signature – a resonance determined by their geometry and composition – that is measured. When the sculpted end of the fiber is inserted into the specimen and the array of particles interacts with its new surroundings, the detected spectrum changes. This change could be a shift in particle resonance induced by changes in the refractive index of the media surrounding the particles. SERS signals from nearby molecules could also be detected. This fiber device could be used for remote detection of analytes in many situations. In addition, it can be easily moved from sample to sample, and sculpted fibers with various resonances can be used on the same sample to perform different measurements.

Compared to commercial surface plasmon resonance (SPR) sensing systems (Biacore AB), our proposed device may be limited in sensitivity to changes in the surrounding refractive index. However, it offers several advantages. One such advantage is that our probe's geometry allows it to be inserted into fluids and specimens. This is desirable for *in-situ* chemical and biological detection. Additionally, our fiber device can be used as a SERS probe, a function not found in conventional SPR detection systems.

As shown in Fig. 1, one possible detection scheme is for the fiber to be connected to one side of a 2x1 fiber optic coupler. A light source and a spectrometer are connected to the other two coupler ends. Light from the source travels down the coupler and into the fiber device, where it interacts with the antenna array. The reflected light spectrum, modified by the array, is detected by the spectrometer.

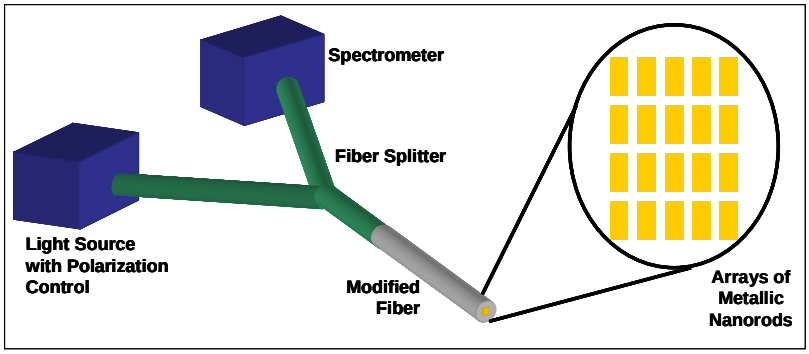

Fig. 1. Schematic of proposed fiber device and its integration into a measurement setup.

3. Arrays

We have carried out a systematic study of the properties of arrays of coupled gold nanorods in order to determine their appropriateness for integration onto the facet of our fiber probe. We decided to study the properties of arrays of nanorods, as they can have strong and broad resonances. This is desirable for SERS measurement as a molecule's SERS signal is proportional to the product of intensities of the surrounding electromagnetic fields at both the pump and the Raman wavelengths [5]. Also, the resonances of arrays are tunable – the rods' length, thickness, width, and spacing are all factors that determine their resonance.

3.1 Simulations

Finite difference time domain (FDTD) simulations were carried out to study the resonances of arrays of metallic nanorods. A single gold rod resting on a 15 nm indium tin oxide (ITO) layer on a silica substrate and surrounded by air on other sides was simulated, using

#82036 - $15.00 USD Received 11 Apr 2007; revised 24 May 2007; accepted 25 May 2007; published 1 Jun 2007

parameters for gold found in Palik [25]. The rod thickness was 50 nm, with varying width and length, and periodic boundary conditions were at the boundaries to create a two-dimensional infinite array of nanorods sitting on the silicon dioxide. In the propagation direction perfectly matched layers (PMLs) were imposed at the boundaries. Light incident on these PMLs undergoes minimal reflection and is quickly attenuated, thus preventing reflections in the simulations which are not present in the experiment. A pulsed excitation polarized along the nanorod's long axis and centered at a wavelength of 690 nm was launched from the air side, normal to the plane of the array. The far-field reflection spectrum was calculated. It was normalized to the input pulse, and the results are shown in Fig. 2.

To study the effects of coupling between gold nanorods along their long axis, simulations were run in which rods 60 nm wide and 140 nm long were separated by 120 nm along their short axis, and 20, 50, 100 and 400 nm along their long axis. As seen in Fig. 2(a), the resonance undergoes a blue-shift from 862 nm to 753 nm as the rod-to-rod gap increases from 20 to 100 nm, but red-shifts to 809 nm when the gap becomes 400 nm.

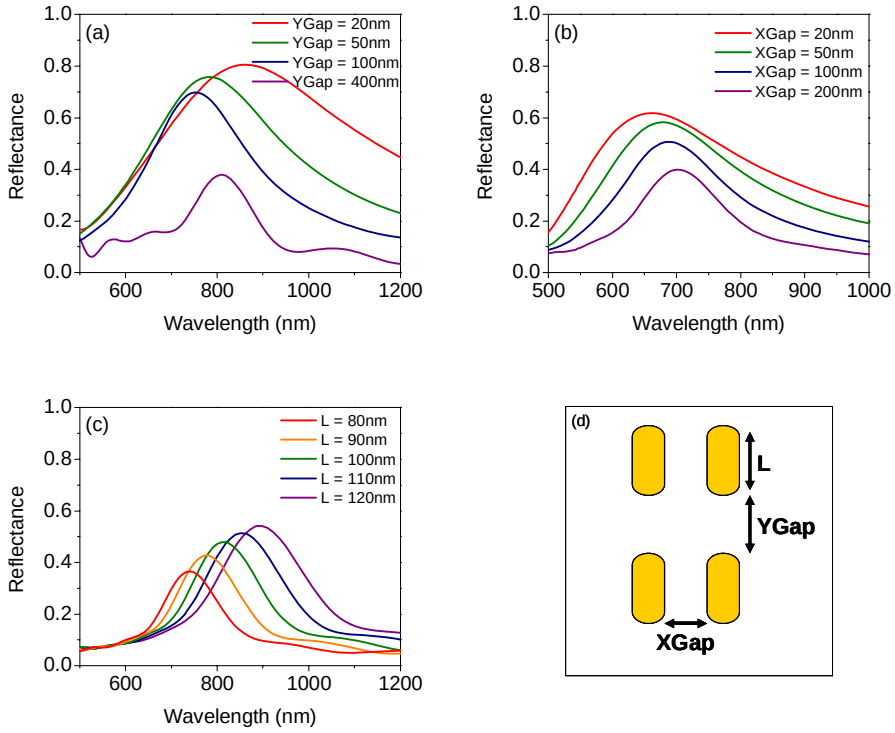

Fig. 2. Results of simulations of resonances for various coupling regimes of the antenna arrays. (a) the gap along the long axis of the rods is changed. As the gap increases from 20 to 50 to 100 nm (red, green and blue curves respectively), a blue-shift occurs. The purple curve, exhibiting a red-shift, shows a resonance when the gap is 400 nm. (b) red shift of the resonant wavelength as the gaps between the rods along their short axis is increased from 20 nm (red), 50 nm (green), 100 nm (blue), to 200 nm (purple). The resonance red-shift in (c) results from increases in the nanorods' length from 80 to 120 nm. (d) geometry of the nanorods arrays.

Coupling between the gold nanorods in the direction along their short axis was studied by simulating rods 80 nm long and 40 nm wide. They were spaced 40 nm apart along their long axis, and 20, 50, 100 and 200 nm apart along their short axis. In this situation, the resonance underwent a red-shift, moving from 662 nm to 704 nm. This is shown in Fig. 2(b).

#82036 - $15.00 USD Received 11 Apr 2007; revised 24 May 2007; accepted 25 May 2007; published 1 Jun 2007

Changing the length of the nanorods was examined by simulating rods 40 nm wide, with a 30 nm separation along their long axis and 310 nm separation along their short axis. Their lengths were varied from 80 nm to 120 nm in increments of 10 nm. As shown in Fig. 2(c), as the rod length increased the resonances of these arrays red-shifted from 738 nm to 895 nm.

The time-averaged electric field intensity at the top surface of the nanorods was also calculated with the FDTD method. Shown in Fig. 3(a) is the resulting intensity profile for a rods 140 nm long and 60 nm wide, separated by a 20 nm gap. A continuous-wave excitation was launched incident onto the nanorods, and its wavelength, 862 nm, was chosen to be the peak of the corresponding resonance shown in Fig. 2(a). A maximum intensity enhancement of ~50 occurs in the small gap between the rods, close to edges of the rods.

3.2 Experimental results

Experimental testing was done by fabricating 100 μm x 100 μm gold nanorod arrays on ITO coated glass slides (Sigma-Aldrich). The slides were spin coated with polymethyl methacrylate (PMMA), and then the arrays were defined using electron-beam lithography. These arrays varied in both nanorod length and rod-to-rod coupling distance. The lithography was followed by electron-beam evaporation of a 3 nm adhesion layer of titanium and a 50 nm layer of gold. A standard lift-off process removed excess metal and left the desired nanorod arrays. A representative image of one of our arrays is shown in Fig. 3(b).

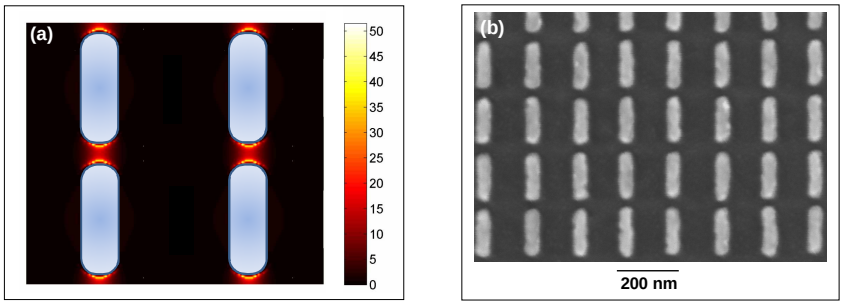

Fig. 3. (a) electric field intensity enhancement at a wavelength of 862 nm. The rods correspond to the red curve in Fig. 2(a), and are 140 nm x 60 nm, separated by a Y-gap of 20 nm and a X-gap of 120nm. (b) micrograph of an array of gold nanorods fabricated on ITO coated glass slides with electron-beam lithography.

The reflection spectrum of the arrays was measured by illuminating the rods with a white light source. The white light was collected from our fiber coupled light source, sent through a polarizer and a 50x microscope objective (Mitutoyo, infinity corrected, NA = 0.55, working distance = 13 mm), which focused the light on the sample. The reflected light that passed back through the microscope objective was collected into a fiber coupled spectrometer. For a reflection reference, a reflection spectrum was taken from a silver mirror inserted in place of the sample. Background light was measured and subtracted from our spectra.

The nanorods in the first set of arrays that we studied were approximately 60 nm wide and 140 nm long. Gaps between the rods in the direction along the rod's long axis were ≈20, 50, 100 and 400 nm. This gap is termed the Y-gap. In the other direction, gaps between the rods were ≈120 nm. Light was incident on the rods polarized in the direction along the long axis. Figure 4(a) shows that as the gap between the rods was increased from 20 to 100 nm, the resonance of the arrays blue-shifted from 740 nm to 693 nm. At a gap of 400 nm the resonance underwent a red-shift. As was the case for all our experimental results, no resonances were measured when the light was polarized along the rod's short axis.

Nanorods that were 80 nm long and 40 nm wide were used to study the coupling between rods in the direction along their short axis. The gaps between the rods were made ≈20, 50,

#82036 - $15.00 USD Received 11 Apr 2007; revised 24 May 2007; accepted 25 May 2007; published 1 Jun 2007

100 and 200 nm, while the gap along their long axis was ≈40 nm. Light was polarized along the rod's long axis. Figure 4(b) shows the red shift that was observed in the measured resonance as the gap, termed the X-gap, was increased. An array with gaps of 20 nm exhibited a resonance at 606 nm, while one with 200 nm gaps was resonant at 653 nm.

Arrays of coupled nanorods with varying length were also examined. The fabricated nanorods were 40 nm wide and varied in length from ≈80 to 120 nm in steps of 10 nm. The gap along the nanorods long axis was ≈30 nm and ≈310 nm along the rods short axis. Figure 4(c) shows the red shift observed as the rods increased in length. The difference in resonance wavelength between the 80 nm and 120 nm long rods was 138 nm.

The resonances of arrays of coupled nanorods were also measured as the index of the material interacting with the near-field of the nanorods was changed. As shown in Fig. 4(d), the measured resonances underwent a red-shift as the index surrounding them was increased. The measured resonance of the array in air was peaked at a wavelength of 670 nm, and it shifted to 709 and 728 nm when immersed in index matching fluid with indices 1.35 and 1.46, respectively. Spectra shown were taken immediately after the index matching fluids were added. Additional reflection measurements, not shown, were taken after the index fluid was allowed to dry. These resonances had increased amplitude, but their peak resonance wavelengths were unchanged from those in Fig 4(d).

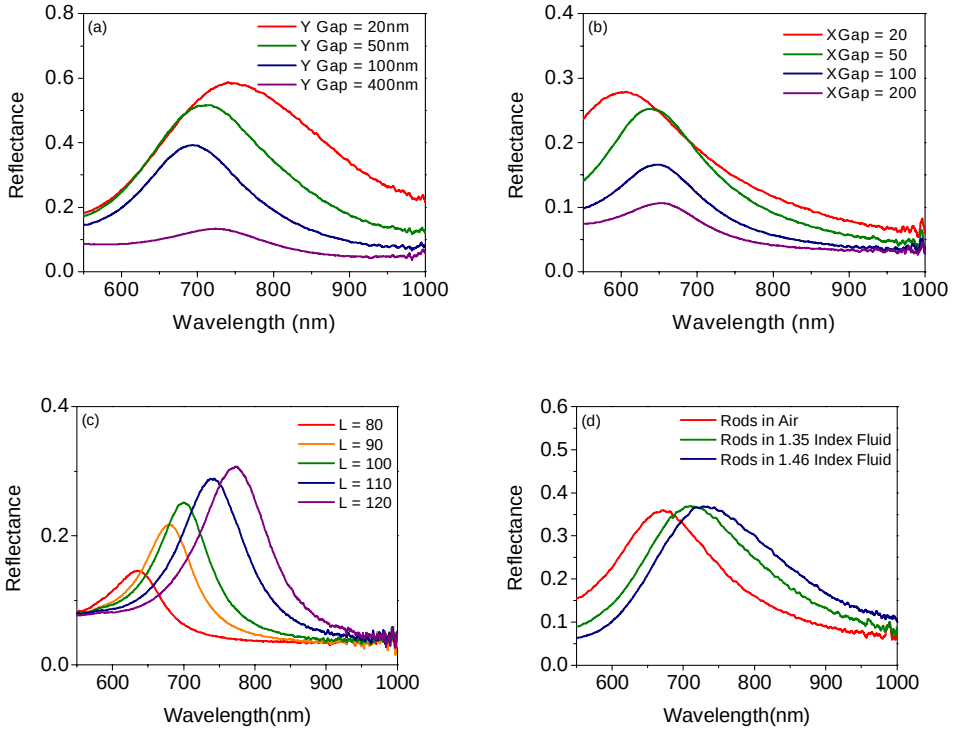

Fig. 4. Measured resonances for various coupling regimes. (a) the gap along the long axis of the rods is changed. A blue-shift occurs as the gap increases from 20 to 50 to 100 nm (red, green and blue lines respectively). The purple line shows a resonance from a gap of 400 nm. The resonance is red-shifted as the gap becomes large enough for the rods to undergo phase retardation. (b) red shift of the resonant wavelength as the gaps between the rods along their short axis is increased from 20 nm (red), 50 nm (green), 100 nm (blue), to 200 nm (purple). (c) red-shift due to increases in the rod length (80 nm to 120 nm), while the rod-to-rod spacing is held constant. The resonance red-shift in (d) is induced by changing the refractive index of the media surrounding the rods from 1.0 (red), to 1.35 (green) to 1.46 (blue).

#82036 - $15.00 USD Received 11 Apr 2007; revised 24 May 2007; accepted 25 May 2007; published 1 Jun 2007

Figure 5 shows a comparison between our experimentally measured shifts in resonance due to changes in nanorod coupling and length. This graph shows that resonance peak position is more sensitive to changes in the length of the nanorods than the size of the gaps between the rods. An increase of 10 nm in nanorod length can shift the resonance of the array by ≈40 nm, whereas an 80 nm increase in the gap between the rods along their long or short axis is needed to achieve this same shift in resonance.

There are some differences between our simulations and experimental measurements. The trends exhibited in each are the same; however the resonances found in our simulations are generally red-shifted, higher in magnitude and narrower than those we measured from nanorods of equal size and spacing. We attribute these discrepancies to differences between the simulations and our experimental situation. Our arrays of fabricated rods have imperfections: electron beam lithography and lift-off leave the rods with slightly different lengths and widths, rough sides and non-uniform heights. Consequently, the gaps in-between the rods vary in size. In the simulations we performed, the rods were all smooth and uniform in shape, and the spacing between the rods was identical. In addition, the light in our experimental setup was focused by a microscope objective and underwent angular divergence. The simulated incident field was normal to the array of rods. Also, our simulations included a 15 nm layer of ITO beneath the metal antennas. In our experiments, the ITO coated slides were purchased with a thickness specified by the manufacturer as 22.5 nm ± 7.5 nm, and thus the ITO thickness varied among the different slides used. These differences resulting from our fabrication process are inherent and all contribute, in different manners and magnitudes, to the various discrepancies found between the measured and simulated reflection spectra.

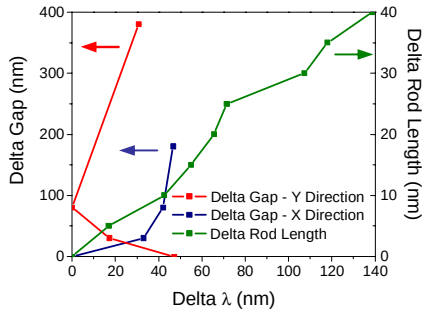

Fig. 5. Comparison of experimentally measured shifts in the peak of resonant wavelength. Shifts due to changes in the gaps between the rods are shown on the axis on the left. In red are shifts due to gap changes in the y direction, and in blue the shifts due to changes in the x direction. The green curve shows shifts in resonance due to changes in nanorod length.

4. Interpretation

The resonances shown in the FDTD simulations and experimental results presented above can be understood by considering the nanorods as radiating dipoles (i.e. antennae). This is valid because at the resonant frequencies the incident light interacts with the nanorods in such a way that they take on a charge distribution that oscillates with the applied field.

In the wavelength range studied, each resonant metal nanoparticle takes on a dipole charge distribution that, at a given time, induces an electric field along the nanorod which adds constructively to the applied field. As the nanorod dipoles oscillate in phase with the applied field, they radiate fields that interact with nearby nanorods. Consider a particular antenna in the array: depending on the spacing and relative position of the neighboring nanorods, the radiated fields from the latter can either add constructively or destructively to the induced fields associated with the antenna's own dipole charge distribution.

#82036 - $15.00 USD Received 11 Apr 2007; revised 24 May 2007; accepted 25 May 2007; published 1 Jun 2007

When considering the interaction of rods along the y-axis (Fig. 2), the fields radiating from nearby nanorods add destructively to the local dipole field. This reduces the force on the electrons in the nanorod, lowering their oscillating frequency (surface plasmon resonance), thus red-shifting the resonant wavelength of a given antenna. When the spacing between the rods along the y direction is increased, the radiating fields from neighboring rods become weaker, blue-shifting the antennas' resonance [26]. This blue-shift is exhibited in three of the curves in Figs. 2(a) and 4(a).

However, as the y-spacing continues to increase, a red-shift of the resonance eventually occurs. This is due to retardation effects in the interaction between neighboring antennae. The electric field that is radiated from one rod propagates to reach neighboring rods. In this configuration, the spacing between the rods is large enough that the radiated field undergoes considerable phase change. When the antenna spacing is such that the phase shift is $\sim \pi$, the radiated fields add constructively with the local dipole field. This results in an increased force on the electrons in the nanorod. In this rod-to-rod spacing range, increasing the separation between the rods results in a decrease of the total field acting on each antenna. This leads to a decrease in the force acting on the electrons in the rods and a red-shift of the resonant wavelength [24]. This red-shift is shown in the purple curve in Figs. 2(a) and 4(a).

In contrast, when examining the interaction of antennas' in the x direction, the fields radiating from nearby neighboring nanorods add constructively to the local dipole field of a particular antenna. This increases the force on the electrons in the rod, increasing the surface plasmon resonance frequency, thus blue-shifting the resonant wavelength. As the rod-to-rod spacing in the x direction increases, these radiating fields decrease in magnitude, causing a red-shift in the resonance spectrum [26]. This is shown in Figs. 2(b) and 4(b).

As the rod length L increases, the antennas' resonant plasmon wavelength increases. This is shown by the red-shift in Figs. 2(c) and 4(c). When the refractive index of the medium in which the antennas are immersed is increased, as in Figs. 4(d), the amplitude of the electric field incident on the nanorods is decreased. This reduces the force on the electrons, slowing down their oscillations and red shifting their resonance.

5. Arrays on fibers

We have studied the properties of coupled nanorod arrays and have verified that they are a suitable choice for integration into our proposed photonic device, a plasmonic optical antenna fiber probe. As demonstrated above, the asymmetry of both the nanorods' geometry and their spacing in arrays allows for easy tuning of the array's resonances. Incorporating them into our devices would allow us to create probes that have resonant responses centered at a specific wavelength.

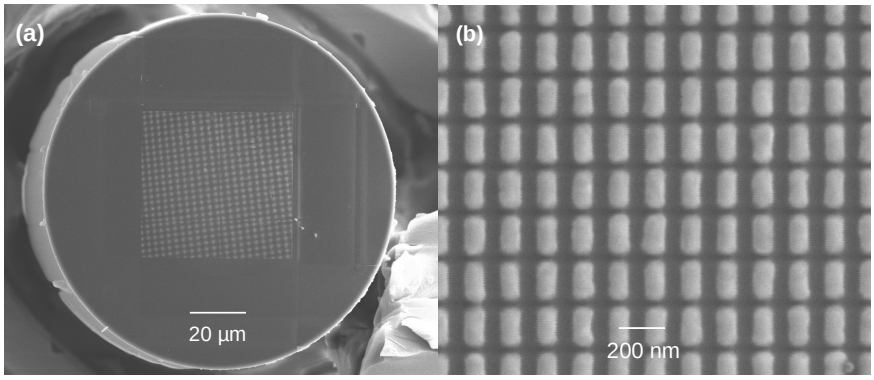

Fig. 6. Facet of a fiber on which an array of coupled nanorods has been fabricated (a). (b) detailed view of the nanorods in the array. Scale bars are 20 µm and 200 nm, respectively.

#82036 - $15.00 USD Received 11 Apr 2007; revised 24 May 2007; accepted 25 May 2007; published 1 Jun 2007

We have developed a method to fabricate such devices using a gallium focused-ion beam (FIB) system. We evaporate a 3 nm sticking layer of titanium and 35 nm of gold on the facet of a fiber, and then use the ion beam to selectively remove the gold and titanium, leaving behind arrays of gold nanorods. To maximize the interaction between the light in the fiber and our nanorods, we position our arrays to cover the core of the fiber. Figure 6 shows an example of a facet of a device that we have fabricated, composed of a 62.5 μm x 62.5 μm array of nanorods, each of which is ≈165 nm x 80 nm, separated by gaps of ≈30 nm along their long axis and ≈80 nm in the perpendicular direction. This array was positioned over the core of the 62.5 μm diameter core of the multimode fiber (GIF625 from ThorLabs). After the array was fabricated, the unsculpted gold remaining around the edges of the fiber was removed with the focused ion beam.

The arrays shown in Fig. 6 are positioned over the core of a multimode fiber, demonstrating that our fabrication technique can be used to create a device that would have a large interaction area with the sample under investigation. In this configuration the light incident on the nanorod array would have components polarized both parallel and perpendicular to the rods' long axis, and thus only some of the incident light would excite the array's resonances. If a smaller interaction area and more efficient use of the incident light were desired, the nanorod array could also be fabricated on the facet of a single mode fiber. With the addition of polarization control of the input light, a device made on standard single mode fiber or polarization maintaining fiber could be used.

6. Conclusion

We have completed a study of coupled optical antenna arrays and confirmed that they are an appropriate choice for integration into our fiber sensor. We have investigated the effects of rod-to-rod coupling, as well as rod length and the index of the surrounding medium, upon the resonance of a given array. Our results show that the resonances of arrays are highly tunable, and that they are more sensitive to changes in rod length than changes in coupling between the rods.

Acknowledgments

This work was supported by AFOSR under Contract No. FA9550-05-1-0435 and by DARPA (Center for Micromechanical and Plasmonic Systems) under Contract No. HR0011-06-1-0044. We acknowledge useful discussions with Kenneth B. Crozier.

#82036 - $15.00 USD Received 11 Apr 2007; revised 24 May 2007; accepted 25 May 2007; published 1 Jun 2007